



INTERNATIONAL ATOMIC ENERGY AGENCY
UNITED NATIONS EDUCATIONAL SCIENTIFIC AND CULTURAL ORGANIZATION



INTERNATIONAL CENTRE FOR THEORETICAL PHYSICS

34100 TRIESTE (ITALY) • P.O.B. 586 • MIRAMARE • STRADA COSTIERA 11 • TELEPHONE: 2240-1
CABLE: CENTRATOM - TELEX 460392 - I

H4.SMR/285 - 31

WINTER COLLEGE ON LASER PHYSICS: SEMICONDUCTOR LASERS AND INTEGRATED OPTICS

(22 February - 11 March 1988)

LINBO₃ OPTICAL WAVEGUIDE FABRICATION BY TI INDIFFUSION
AND PROTON EXCHANGE: PROCESS, PERFORMANCES AND STABILITY

R.M. De La Rue
Glasgow University
Glasgow, U.K.

LiNbO₃ optical waveguide fabrication by Ti indiffusion
and proton exchange: process, performances and stability

C. Canali⁺, A. Carnera^{*}, P. Mazzoldi^{*} and R.M. De La Rue⁺⁺

⁺ Istituto di Elettrotecnica ed Elettronica dell'Università
Via Gradenigo 6/A, 35131 Padova, Italy

^{*} Dipartimento di Fisica dell'Università, Via Marzolo 8, 35131 Padova, Italy

⁺⁺ Department of Electronics and Electrical Engineering,
Glasgow G12 8QQ, Scotland, U.K.

Abstract

Correlations between optical properties and structural modifications induced by the fabrication procedures are reported for both Ti indiffused and proton exchanged LiNbO₃ waveguides. Surface roughness and structural defects account for the dependence of the propagation losses on the diffusion time in Ti:LiNbO₃ waveguides. The heavy lattice distortion induced by the high H concentration is related to the high in-plane scattering levels in proton exchanged waveguides. Post annealing reduces lattice distortions and improves optical performances.

Introduction

LiNbO₃ is an electro-optical material of current interest for the fabrication of guided wave devices such as switches, modulators, wavelength multiplexers and demultiplexers.¹ The essential element of these devices is an optical waveguide consisting of a higher refractive index layer, few microns in thickness at the surface of a LiNbO₃ crystal with a patterned stripe geometry.

Among different fabrication methods the most firmly established waveguide fabrication technology in LiNbO₃ is the indiffusion of Ti atoms while recently a remarkable interest has been devoted to the proton exchange technology^{2,3} which allows to obtain a higher increase of the extraordinary refractive index.

Waveguide quality is of vital importance for the performances of all guided-wave optical devices and it is clear that the quality, performances and long term stability of the waveguides are connected with their fabrication process. Nevertheless a complete and systematic study of the relation between waveguide optical properties and fabrication process does not appear to have been published up to now. This paper describes results of such a study restricted to two main aspects: i) the correlation between optical properties and crystalline defects induced by the fabrication process, ii) long term or thermal stability of proton exchanged waveguides. To do that LiNbO₃ waveguides fabricated by Ti indiffusion process and proton exchange in pure melted benzoic acid were optically and structurally characterized. Optical properties, waveguide effective modes and inferred index-depth profiles and in-plane scattering levels, were mainly analysed by the two prisms coupler method at the He-Ne wavelength^{4,5,6} while structural properties were studied by means of various microanalytical techniques giving atomic composition profiles, crystalline nature and quality of the waveguiding layer.^{7,8,9}

Results to be presented will indicate the nature of the structural modifications occurring within the waveguide region and at its surface, and these will be compared with measurements of refractive index and/or of in-plane scattering levels. Similar data have been obtained on well polished optical-grade LiNbO₃ substrate with different crystallographic orientations supplied by Crystal Technology Inc. and Barr and Stroud Ltd. This similarity indicates that the observed effects and the correlations between optical and structural properties of the examined waveguides are dominated by the fabrication procedure and not by slight differences in substrate quality and stoichiometry.

Ti indiffused waveguides

Thin Ti films were deposited by sputtering or by electron beam evaporation on LiNbO₃ substrates and indiffused at 1000°C in flowing gas^{7,8,9}. Either O₂ and N₂ flowing dry and wet

atmospheres (i.e. bubbled through a 30 cm high column of water heated at 90°C before entering in the diffusion furnace) have been used. The heating and cooling rates were both 30°C/min, so that only the time, t_d (1:50 hrs), spent at the steady diffusion temperature, $T_d = 1000^\circ\text{C}$, is significant and therefore used as a basis of comparison in this paper.

Using all substrate crystallographic orientations and atmospheres during Ti indiffusion it was found that there is a typical characteristic behaviour in the dependence of in-plane scattering levels, ΔI (dB/cm), on the diffusion time t_d . In fact for a given initial Ti thickness by increasing t_d , the value of ΔI first decreases steadily to a minimum and then eventually increases again. Fig. 1 reports this typical behaviour for two series of waveguides fabricated on Y-cut oriented substrates starting from two initial thicknesses of the Ti film: 250 and 550 Å respectively. Furthermore the dependence of ΔI on t_d is similar when measured for both TE_0 and TM_0 propagation modes in the same waveguides series. These similarities suggest that this characteristic behaviour should be directly related to the Ti indiffusion process and to the time evolution of imperfections produced in the waveguide region.

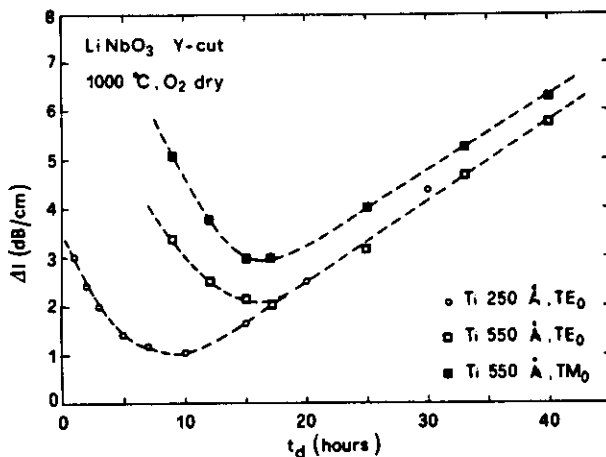


Figure 1. In plane scattering levels (ΔI) vs t_d at 1000°C for TE_0 and TM_0 modes in samples coated with 250 Å and 550 Å thick Ti films.

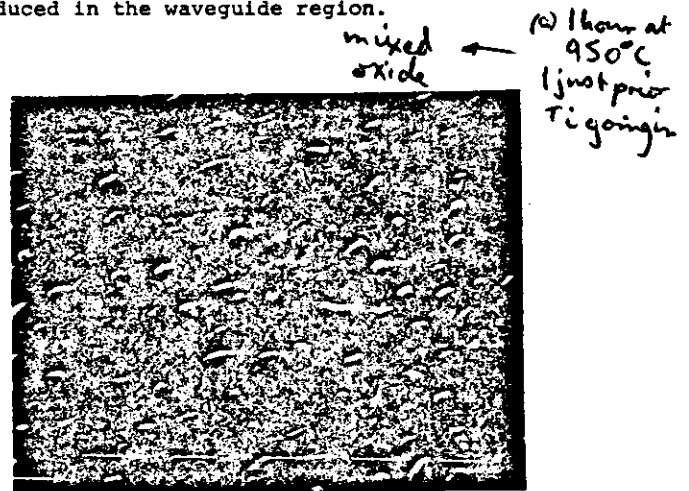


Figure 2. SEM micrograph of surfaces of a 950°C, 10 hr annealed in dry O_2 sample. White markers are 1 μm long.

Waveguide in-plane scattering⁶ may be mainly caused by: i) non-uniformities in the Ti diffusion occurring at the surface and within the waveguide region, ii) roughness at the waveguide surface, iii) strains and crystallographic defects induced in the guiding region. All of these causes must be considered in the case of Ti-diffused LiNbO_3 waveguides.

Recent investigations^{7,8,9} of the Ti-indiffusion process have shown the following features:

- during the initial warm-up process, Ti oxidizes at about 500°C.
- In dry atmosphere the LiNb_3O_8 phase appears at about 600°C, grows, reaches a maximum amount at about 800°C and then decomposes rapidly. LiNb_3O_8 formation is inhibited when Ti indiffusion is performed in wet atmosphere.
- After the appearance of LiNb_3O_8 phase, the $x\text{TiO}_2-(1-x)\text{NbO}_2$ mixed oxide with $x=0.65$ also begins to grow, and it is the only phase present at 900°C behaving as the real source for the subsequent Ti-indiffusion process.
- As annealing at 1000°C continues, Ti diffuses from the surface layer into the underlying LiNbO_3 substrate and consequently the $(\text{Ti}_{0.65}\text{Nb}_{0.35})\text{O}_2$ phase eventually disappears. Islands of the mixed oxide are always detectable by scanning electron microscopy (SEM) just before their complete consumption, as shown in Fig. 2, indicating a non-uniform indiffusion process. The presence of these islands causes a roughness of the surface of the waveguides. We expect that for longer values of the diffusion time, t_d , non uniformities within Ti-diffused LiNbO_3 due to the earlier existence of $(\text{Ti}_{0.65}\text{Nb}_{0.35})\text{O}_2$ islands decrease as indicated by the reduction of in-plane scattering levels. In fact lateral and in depth diffusion of Ti atoms with increasing t_d may relieve these non-

much slower
(similar to 1000°C, ~10 hrs)

uniformities. At the same time the surface roughness decreases monotonically with increasing t_d with an approximately $t_d^{-1/2}$ dependence suggesting that a diffusion process controls the decrease of the surface roughness.

These effects discussed in d) imply a reduction of the level of light scattering induced by inhomogeneities of refractive index and by surface roughness as t_d increases. The subsequent increase of in-plane scattering levels, observed for longer diffusion times t_d , may be explained by the observed increase of the density of the crystalline defects induced in the guiding region by the Ti indiffusion process. In fact Ti^{4+} ions have a ionic radius of 0.67 Å lower than that of Nb^{5+} ions, 0.70 Å, whose lattice sites they tend to occupy. As a consequence the indiffusion of Ti ions will induce a lattice negative strain (contraction) in the indiffused layer^{10,11}. Figure 3 shows the relation between Ti concentration and the strain values ($\epsilon_y = -\Delta a/a$) measured by using an electron microprobe and a double crystal X-ray diffractometer respectively. This strain can be relieved by the inset of crystalline defects, whose density and nature can be revealed by X-ray topography (XRT) and transmission electron microscopy (TEM).

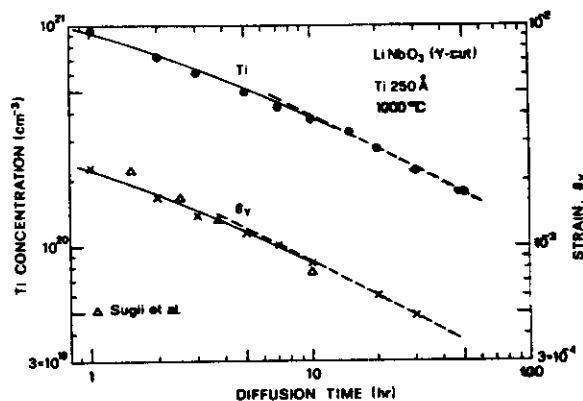


Figure 3. Surface Ti concentration and strain as a function of diffusion time.

Figure 4 reports X-ray topographs from samples of the 250 Å-Ti series of Fig. 1. The excess diffraction contrast observed in Fig. 4 increases as t_d increases and this is attributable to an increase in the density of misfit dislocations which are probably generated at the interface between the Ti diffused layer and the substrate. The dislocations are clearly caused by the Ti indiffusion. In fact regions not coated with Ti appear to be quite free of dislocations as can be seen in Fig. 4d. A misfit dislocation network well resolved in Fig. 4b appears for $t_d=5$ h. The dislocation density increases with increasing t_d up to a relatively high value ($\approx 10^5/cm^2$) when the single dislocations can no more be resolved by the technique. Further evidences indicating that the number of defects increases in samples heated for prolonged periods have been obtained by TEM experiments. Figures 5 and 6 show TEM micrographs and electron diffraction patterns taken on samples of the 250 Å-Ti series shown in Fig. 1. On the sample annealed for 1 hour, corresponding to an optical in-plane scattering level of 3 dB/cm, we observed (Fig. 5a) the presence in various regions of a discontinuous surface layer which gives the images of a characteristic rough aspect typical of the final stage of the non-uniform consumption of the mixed oxide layer. Figure 5b shows the appearance of traces corresponding to preferential cleavage orientations, mainly evidenced as parallel to the $[104]$ direction observed in the samples annealed for 1 hour. The different zones present in this image are the results of the first stage of a process which will become more evident in the samples thermally treated for longer times: it consists in the gradual formation of adjacent crystal zones where orientations differ by small rotation angles. These traces are the so called "small angle grain boundaries". It is well known that along such boundaries we encounter a set of essentially edged-type dislocations like the one clearly visible in Fig. 5c. The final stage of the process is shown in Fig. 6. Figure 6a reports a TEM image taken from a sample annealed for 50 hrs which optically exhibits a 10 dB/cm in-plane scattering level (Fig. 1). The image shows a very high density of defects and a severely damaged crystal structure. In the corresponding diffraction pattern (Fig. 6b) we can distinguish many "multiple" spots denoting the tendency to a polygonalization and/or twinings.

Both TEM and XRT results strongly evidence a formation of crystalline defects in the wave

5a: black is too thick for transmission, ($\sim 100,000$ Mag) composition variation
white is transparent (depth + surface)

5b. 104 is standard cleavage plane, 2H reference

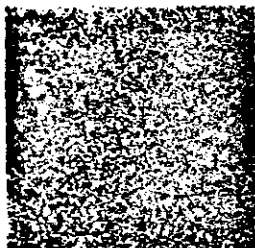
5c. g (Burger's vector) — dislocation loop along boundary.

defects → black.
and film scan sample
Lang camera (reflection geometry)
each line is many dislocations (spirals) (loops)

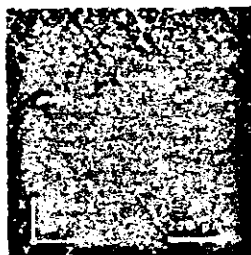
104
60
grain boundaries
(orientation? checked by diffraction)

Ti (250 Å) / LiNbO₃ (Ycut) 1000 °C O₂ dry

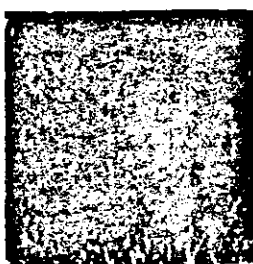
a) $t_d = 1h$



b) $t_d = 5h$



c) $t_d = 50h$



d) $t_d = 50h$



Figure 4. X-ray topographs (Cu K α_1 radiation, (030) reflection) of three samples annealed at 1000°C for different times. (d) is a topograph of a sample only partially coated by Ti. Magnification is the same in (a), (b), (c) and (d).

guiding region which are induced by the Ti indiffusion process itself and whose density increases with increasing diffusion time. This increasing defect density accounts for the increasing levels of in-plane scattering in samples diffused for prolonged periods.

Proton exchanged waveguides

The main advantage of proton exchange fabrication process of LiNbO₃ optical waveguides consists in the higher values of the extraordinary index which can be readily obtained by this technique^{2,3}. On the other hand the waveguides exchanged in pure benzoic acid show relatively high in-plane scattering levels^{3,12} and long term and/or thermally activated variation of optical parameters^{13,14}. In fact a refractive index decrease in waveguides stored at room temperature have been reported¹³. Furthermore the work by De Micheli and co-workers¹⁵ had already shown that a relatively low temperature thermal treatment can rapidly modify the index profile and help in giving control over waveguide properties. There is a clear need for a further structural study of either waveguide formation process and of the annealing effect in order to obtain a better control of the optical performances of the waveguides.

As already reported¹⁶ nuclear reactions (NR) allow a direct measurement of the H concentrations and profiles in the exchanged layer. These measurements showed step-like H profiles with more than 10^{22} H ions per cm³ in the constant concentration zone in broad agreement with data reported by Jackel et al.¹⁷ Such a high H concentration induces a severe distortion in the host lattice which can be measured by double crystal X-ray diffraction. Figure 7 shows double crystal X-ray diffraction, (220) rocking curve, taken on X-cut samples isochronally (40 min) exchanged in pure benzoic acid at four different temperatures. One can see from the presence of satellite peaks at negative deviations ($\Delta\theta$) from the Bragg angle relative to the unperturbed substrate, that the exchanged layer exhibits a positive strain $\Delta a/a$. Positive strains have been observed also to happen for analogous treatments in z-cut and y-cut LiNbO₃ crystals. The shape and position of the satellite peaks remain the same with increasing the exchange temperature while their intensities increase linearly, as expected, as a function of the exchanged layer thickness. This lattice distortion is clearly visible also by Ruther-

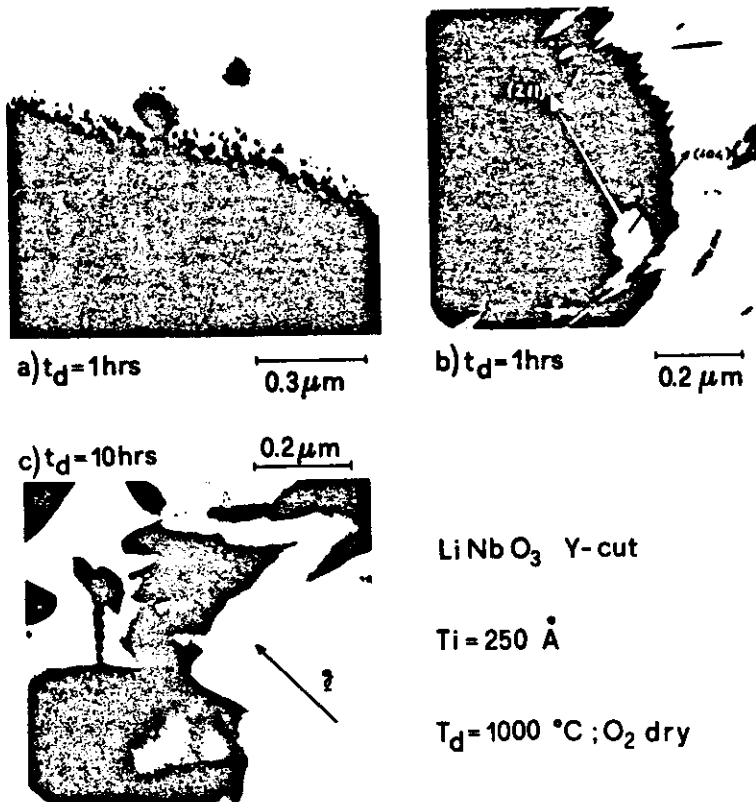


Figure 5. Transmission electron micrographs of samples annealed at 1000°C for 1 and 10 h respectively.

LiNbO₃ Y-cut; Ti-250 Å; $T_D = 1000^\circ\text{C}$; O₂ dry, $t_D = 50 \text{ hrs}$

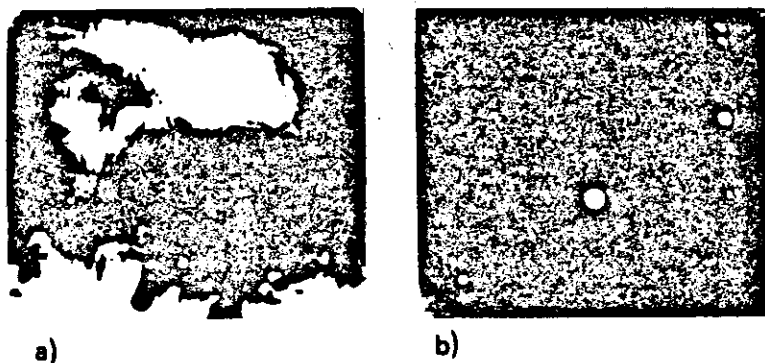


Figure 6. a) Transmission electron micrographs of a sample annealed at 50 h. b) Electron diffraction patterns of the same area shown in a).

ford backscattering spectrometry (RBS) in channeling conditions, thus allowing the evaluation of the thickness of the distorted layer. The thicknesses measured by optical methods, nuclear reactions and RBS will agree each other thus suggesting a close correlation between the presence of a high H concentration, the lattice distortion and the increase of the refractive index in the waveguiding layer. Thermal treatments of the exchanged waveguides induces: i) changes in the refractive index values and in their profiles from simple step like towards gaussian-type; ii) similar changes in the profiles of H and of lattice distortion; iii) reduction of the in-plane scattering levels; iv) reordering of the crystal structure in

the waveguiding region.

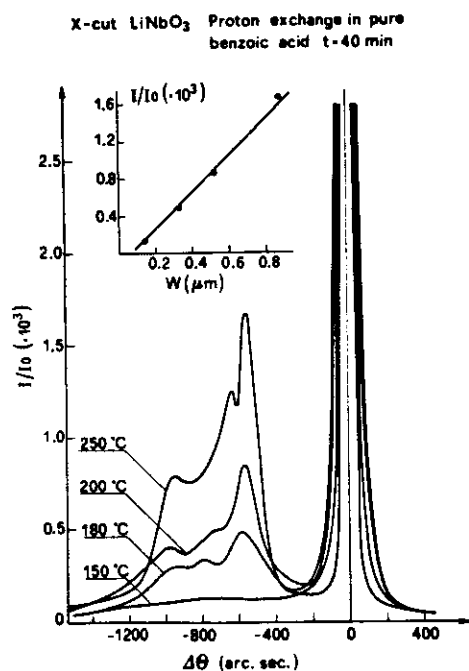


Figure 7. Double crystal (220) rocking curves on X-cut isochronally proton exchanged in pure benzoic acid. Insert show the satellite peak amplitude vs exchanged layer thickness.

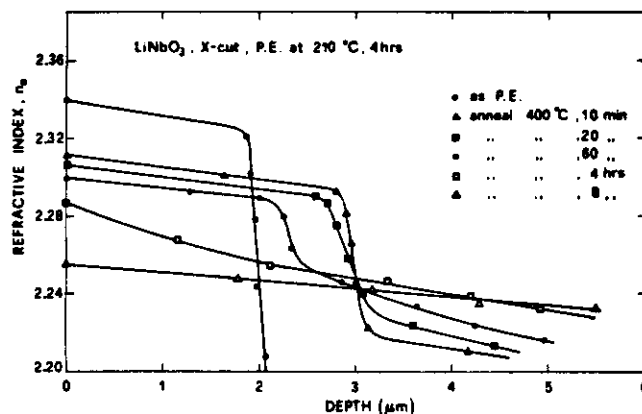


Figure 8. Refractive index, n_e , vs depth profile on X-cut samples P.E. and isothermally annealed.

Figure 8 gives the refractive index versus depth profile in X-cut LiNbO_3 samples proton exchanged for 4 hours at 210°C and then isothermally annealed in flowing O_2 . The inverse WKB method³ was used in constructing these profiles. Variations in the annealing time clearly produce major differences in the shape of the refractive index profiles. Figure 9 shows the results of RBS observations on X-cut samples proton exchanged and isochronally annealed at 325°C . RBS spectra taken in aligned conditions show an increase in the backscattering yield, suggesting distortions of the lattice.

The effects of the annealing process are very similar in Figs. 8 and 9, and can be divided in three stages. At a first stage the index profile keeps a step-like shape with an increased thickness and lower value of n_e . Similarly the lattice distortions observed by RBS decrease and propagate deeper inside into the bulk. Afterwards for intermediate annealing periods the constant n_e layer thickness decreases due to the hydrogen indiffusion which gradually reduces the constant hydrogen concentration layer at the interface with the substrate. The guiding profile remains mainly step like with a long tail. The same "erosion" and thinning of the distorted layer are observed in the RBS spectra. For longer annealing periods (or higher temperatures) we expect that the H goes deeper and deeper into the substrate and the guide has no more a step-like shape becoming similar to a gaussian diffusion profile. The previously described behaviour agrees with the data obtained by double crystal X-ray diffraction. Figure 10 shows rocking curves from a series of X-cut samples proton exchanged and then isochronally (30 min) annealed at increasing temperatures.

The effect of the first annealing stage is reflected in the strong modification from the broad and low intensity satellite peak produced by the as exchanged sample to the sharp and

high peak observed in the 250°C, 30 min annealed sample. The shape of this latter peak indicates a unique and well defined strain value (0.6%) with a step like in-depth profile. After further increase of the annealing temperature the height of the satellite peak gradually decreases and a tail appears at the left side of the peak relative to the unperturbed substrate. This feature indicates that the sample layer characterized by the maximum strain decreases in thickness and regions with lower strains are formed. In other words the strain profile is smoothed out similarly to the refractive index, Fig.8, and distortion profiles, Fig. 9.

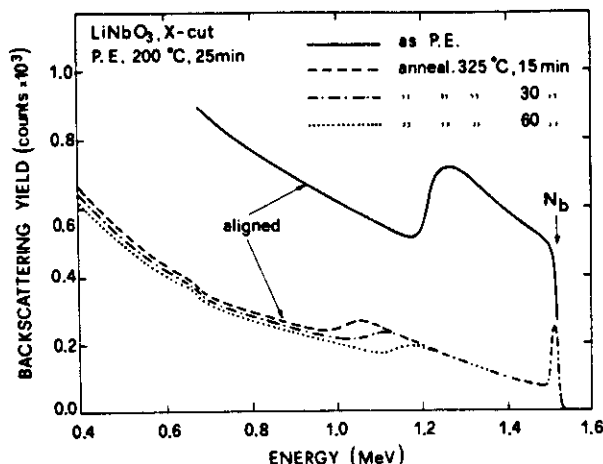


Figure 9. RBS aligned spectra of X-cut samples P.E. and isothermally annealed.

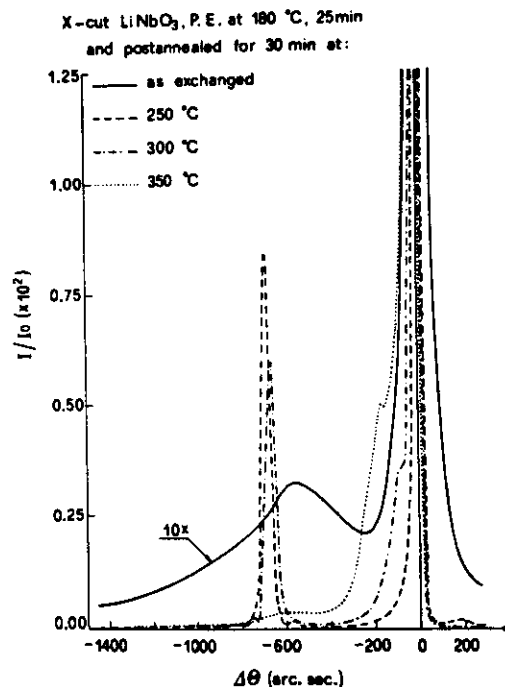


Figure 10. Double crystal (220) rocking curves on X-cut samples P.E. and isochronally annealed.

The data reported point out some peculiarities of the proton exchange process in pure benzoic acid. In the as-exchanged samples the "abrupt" introduction of a large amount of hydrogen causes a heavy and inhomogeneous distortion of the host lattice thus justifying the high observed in-plane scattering levels. At the beginning of the annealing treatment the major phenomenon seems to be an overall reordering of the structure of the guiding layer which maintains a step like profile indicating that the hydrogen atoms do not diffuse deeply in the substrate. This reordering seems to be the cause of the decrease of the light scattering levels.¹⁸ In the samples annealed for longer times (or higher temperatures) the diffusion mechanism becomes predominant driving the hydrogen atoms deeper and deeper in the substrate. Consequently the surface concentration of H decreases, the strain values inside the guiding layer are reduced but the waveguide loses the original sharp profile and supports a higher number of modes.

Conclusions

The performed analysis of waveguides produced in LiNbO_3 by Ti indiffusion and proton exchange in pure benzoic acid demonstrates the requirement for close comparisons between optical and structural studies of the fabricated waveguides in order to obtain a clear understanding of the process, to optimize the waveguide performances, to tailor the fabrication process and to improve the reliability of the device. In particular for Ti indiffused waveguides the

existence of an optimum diffusion time for a given Ti film thickness and diffusion temperature has been demonstrated and explained. For shorter or longer t_d the defects introduced along the fabrication process degrade the properties of the waveguide.

In waveguides produced by proton exchange in pure benzoic acid the high propagation losses are due to the high-density of crystal defects introduced during the H^+Li^+ exchange process. Even annealing for as little as 30 min at 200°C greatly reduces the lattice distortions and propagation losses. On the other hand the high tendency of H to diffuse even at low temperature causes these waveguides to present variations of optical parameters even if stored at room temperature.

Post-annealing of the exchanged waveguides seems to be potentially beneficial also from this latter point of view producing more stable lattice structures and smoothing the H concentration gradient at the waveguide/substrate interface. Furthermore the post-annealing technique allows to modify the guide index profile to optimize input and output coupling to fibers and coupling between parallel stripe guides.

References

1. Alferness, R.C., "Guided-Wave Devices for Optical Communications", IEEE J. Quant. Electron, QE-17, pp. 946-959. 1981.
2. Jackel, J.L., Rice, C.E. and Vasselka, J.J., "Proton Exchange for High Index Waveguides in $LiNbO_3$ ", Appl. Phys. Lett., 41(7), pp. 607-608. 1982.
3. Clark, D.F., Nutt, A.C.G., Wong, K.K., Laybourn, P.J.R. and De La Rue, R.M., "Characterization of Proton Exchange Slab Optical Waveguides in Z-Cut $LiNbO_3$ ", J. Appl. Phys., 54, pp. 6218-6220. 1983.
4. Tien, P.K., Ulrich, R., "Theory of Prism Coupler and Thin Film Light Guides", J. Opt. Soc. Amer., 60(10), pp. 1325-1337. (1970).
5. Sarid, D., Cressman, P.J., Holman, R.H., "High-Efficiency Prism Coupler for Optical Waveguides", Appl. Phys. Lett., 33(6), pp. 514-515 (1978).
6. Vahey, D.W., Verber, C.M., Wood, V.E., "Sources of Scattering of Guided Light in Ti-Diffused $LiNbO_3$ Optical Waveguides", Ferroelectrics, 27, pp. 81-84. 1980.
7. Armenise, M.N., Canali, C., De Sario, M., Carnera, A., Mazzoldi, P. and Celotti, G., "Characterization of $(Ti_{0.65}Nb_{0.35})O_2$ Compound as a Source for Ti Diffusion during $Ti:LiNbO_3$ optical waveguide fabrication", J. Appl. Phys., 54, pp. 62-70. 1983.
8. Armenise, M.N., Canali, C., De Sario, M., Carnera, A., Mazzoldi, P. and Celotti, G., "Characterization of TiO_2 , $LiNb_3O_8$ and $(Ti_{0.65}Nb_{0.35})O_2$ Compound Growth observed during $Ti:LiNbO_3$ Optical Waveguide Fabrication", J. Appl. Phys., 54, pp. 6223-6231. 1983.
9. De Sario, M., Armenise, M.N., Canali, C., Carnera, A., Mazzoldi, P., Celotti, G., " TiO_2 , $LiNb_3O_8$ and $(Ti_xNb_{1-x})O_2$ Compound Kinetics during $Ti:LiNbO_3$ Waveguide Fabrication in Presence of Water Vapours", to be published on J. Appl. Phys.
10. Armenise, M.N., Canali, C., De Sario, M., Franzosi, P., Singh, J., Hutchins, R.H., De La Rue, R.M., "The Dependence of In-Plane Levels in $Ti:LiNbO_3$ Optical Waveguides on Diffusion Time", to be published on IEEE-H Proc. Microwaves, Optics and Antennas.
11. Sugii, K., Furuma, M. and Iwasaki, H., "A Study on Ti Diffusion into $LiNbO_3$ Waveguides by Electron Probe Analysis and X-Ray Diffraction Methods", J. Mater. Science, 13, pp. 523-533. 1978.
12. Armenise, M.N., Al-Shukri, S.M., Dawar, A., De La Rue, R.M. and Nutt, A.C.G., "Optical Characterization of proton exchanged and Titanium-Diffused Proton Exchanged Slab Waveguides on Lithium Niobate", Proc. of Intern. Workshop on Integrated Optical and Related Technologies for Signal Processing, Florence, Italy September 1984, p. 21.
13. Yi-Yan, A., "Index Instabilities in Proton-Exchanged $LiNbO_3$ Waveguides", Appl. Phys. Lett., 42(8), pp. 633-635. 1983.
14. Al-Shukri, S.M., Dawar, A., De La Rue, R.M., Nutt, A.C.G., Taylor, M., Tobin, J.R., Mazzi, G., Carnera, A. and Summonte, C., "Analysis of Annealed Proton Exchanged Waveguides on Lithium Niobate by Optical Waveguide Measurements Microanalytical Technique", Post-Dead Line Paper, Presented at 7th Top.Meet. on Integrated and Guided Wave Optics, Kissimmee, Florida, April 1984. PD71-4.
15. De Micheli, M., Botineau, J., Neveu, S., Sibillot, P., Ostrowsky and Papuchon M., "Independent Control of Index and Profiles in Proton-Exchanged Lithium Niobate Guides", Optics Lett., 8, pp. 114-115. 1983.
16. Canali, C., Carnera, A., Della Mea G., De La Rue, R.M., Nutt, A.C.G. and Tobin, J.R., "Proton Exchanged $LiNbO_3$ Waveguides: Material Analysis and Optical Characteristics", SPIE,

Vol. 460 paper O7 (1984), SPIE Meeting, Los Angeles, January 1984.

17. Jackel, J.L., Rice, C.E. and Veselka, J.J., "Composition Control in Proton Exchanged LiNbO_3 ", Electronics Letters, 19, pp. 387-388. 1983.

18. Dawar, A., Al-Shukri, S.M. and De La Rue, R.M., Surface Acoustic Wave-Guided Optical Wave Interaction in Y-Cut LiNbO_3 Annealed Proton-Exchanged Waveguides, Post dead-line paper presented at Intern.Workshop on Integrated Optical and Related Technologies for Signal Processing, Florence, Italy, September 1984.